ATMOSPHERIC MODELS FOR AEROENTRY AND AEROASSIST

C. G. Justus[1], Aleta Duvall[1], and Vernon W. Keller[2]

[1]NASA MSFC ED44/Morgan Research, Marshall Space Flight Center, AL 35812 (USA),
Jere.Justus@msfc.nasa.gov, Aleta.Duvall@msfc.nasa.gov
[2]NASA Marshall Space Flight Center, ED44, Marshall Space Flight Center, AL 35812 (USA),
Vernon.Keller@nasa.gov

ABSTRACT

Eight destinations in the Solar System have sufficient atmosphere for aeroentry, aeroassist, or aerobraking/aerocapture: Venus, Earth, Mars, Jupiter, Saturn, Uranus, and Neptune, plus Saturn's moon Titan. Engineering-level atmospheric models for Earth, Mars, Titan, and Neptune have been developed for use in NASA's systems analysis studies of aerocapture applications. Development has begun on a similar atmospheric model for Venus. An important capability of these models is simulation of quasi-random perturbations for Monte Carlo analyses in developing guidance, navigation and control algorithms, and for thermal systems design. Characteristics of these atmospheric models are compared, and example applications for aerocapture are presented. Recent Titan atmospheric model updates are discussed, in anticipation of applications for trajectory and atmospheric reconstruct of Huygens Probe entry at Titan. Recent and planned updates to the Mars atmospheric model, in support of future Mars aerocapture systems analysis studies, are also presented.

1. INTRODUCTION

Engineering-level atmospheric models have been developed, or are under development, for five of the eight possible Solar System destinations where aerocapture could be used. These include Global Reference Atmospheric Models (GRAMs) for Earth (GRAM-99) [1, 2], Mars (Mars-GRAM 2001) [3-6], Titan (Titan-GRAM) [7], Neptune (Neptune-GRAM) [8], and Venus-GRAM (under development). Physical characteristics of the various planetary atmospheres vary significantly. Likewise, significant variation is found in the amount of available data on which to base the respective engineering-level atmospheric models. The detailed characteristics of these models differ accordingly.

Earth-GRAM is based on climatology assembled from extensive observations by balloon, aircraft, ground-based remote sensing, sounding rockets, and satellite remote sensing. Details are provided in the GRAM User's Guide [1]. Mars-GRAM is based on climatologies of General Circulation Model (GCM) output, with details given in the Mars-GRAM User's Guide [3]. Mars-GRAM has been validated [4-6] by comparisons against observations made by Mars Global Surveyor, and against output from a separate Mars GCM. In contrast, data used to build Titan-GRAM and Neptune-GRAM are more limited, deriving primarily from Voyager observations and limited ground-based stellar occultation measurements. Titan-GRAM is based on data summarized in [9], while Neptune-GRAM was built from summaries of data contained in [10]. For Venus, a substantial amount of data has been collected from orbiter and entry probe observations. These have been summarized in the Venus International Reference Atmosphere (VIRA) [11], which forms the basis for Venus-GRAM (under development).

Fig. 1 shows the wide variety of temperature profiles encountered among the planets and Titan. For Earth, Venus, Mars, and Titan, height is measured from a reference surface (mean sea level on Earth). On Neptune, height is measured above the level at which pressure is one bar (Earth normal sea-level pressure). All of the planets exhibit a troposphere region, where temperature decreases with altitude, indicative of heat flow upward from the surface (on average). All of the planets exhibit a thermosphere region, where (on average) temperature increases with altitude, because of absorption of heat flux from the Sun as it penetrates into the atmosphere. All of the planets have stratospheres, where temperature decrease above the surface diminishes, and remains relatively constant until the base of the thermosphere (Earth being the exception to this, where the presence of ozone and resultant atmospheric heating produces a local temperature maximum in Earth's stratosphere-mesosphere region).

For interest in aerocapture or aerobraking, atmospheric density is the most important parameter. Fig. 2 compares density profiles on the planets and Titan. Vertical dashed lines in Fig. 2 indicate typical density values at which aerocapture or aerobraking operations would occur. Intersections of the aerocapture dashed line with various density curves shows that aerocapture would occur at a wide range of altitudes at the various destinations, varying from about 50 km at Mars to about 300 km at Titan. Aerobraking at Earth, Mars, and Venus would take place near, and just above, the 100 km level. At Neptune and Titan, aerobraking would be implemented near 550 km and 750 km, respectively.

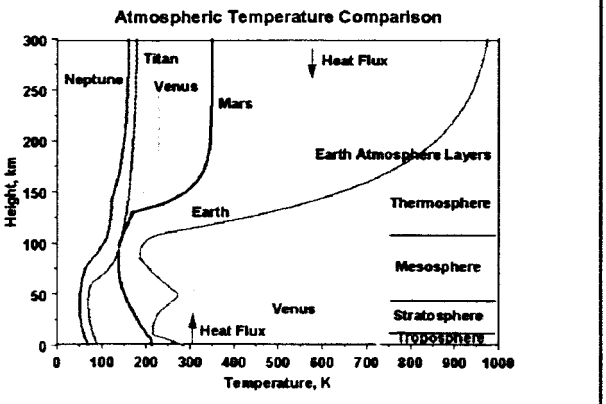

Fig. 1. Comparison of temperature profiles among the planets and Titan.

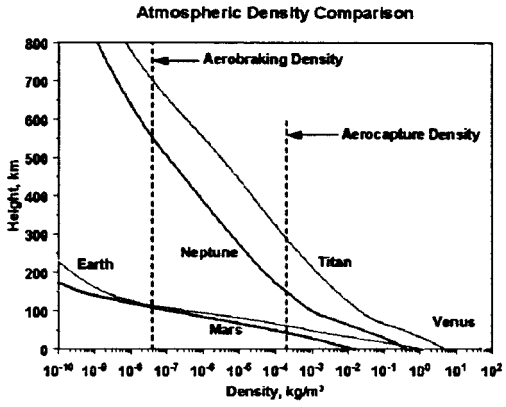

Fig. 2. Comparison of density profiles among the planets and Titan

Fig. 2 shows that density decreases fairly rapidly with altitude for the terrestrial planets (Venus, Earth, Mars), while it decreases rather slowly for Neptune and Titan. This effect is explained by differences in density scale height, H, for the various planets and Titan. Density decreases rapidly with altitude if H is small, while it decreases slowly if H is large. H is proportional to pressure scale height [$R\,T\,/\,(\,M\,g\,)$]. For the terrestrial planets, molecular mass M is large ($M \approx 29$-44), so H is small. On Neptune, H is large because M is small for Neptune's hydrogen-helium atmosphere ($M \approx 2$). For Titan, H is large despite the high molecular mass of its atmosphere ($M \approx 29$), because its gravity is low.

2. BASIS FOR THE ATMOSPHERIC MODELS

In Earth-GRAM, Mars-GRAM, and Venus-GRAM, input values for date, time, latitude, longitude, etc. are used to calculate planetary position and solar position. In this manner, effects of latitude variation and seasonal and time-of-day variations can be computed explicitly. A simplified approach is adopted in Titan-GRAM and Neptune-GRAM, whereby these effects (as well as effects of relatively large measurement uncertainties for these planets) are represented within a prescribed envelope of minimum-average-maximum density versus altitude. Fig. 3 shows this envelope for Titan. Engineering atmospheric model data developed for the Huygens entry probe [9] are used to define the Titan envelope. For Neptune, data from [10] are employed to generate a comparable minimum-maximum envelope, as shown in Fig. 4.

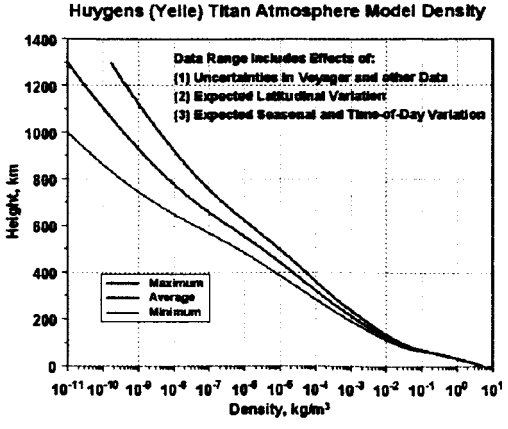

Fig. 3. Minimum, average, and maximum density profiles for Titan [9].

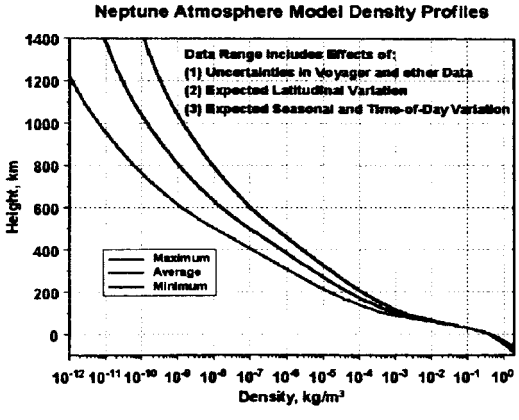

Fig. 4. Minimum, average, and maximum density profiles for Neptune from data in [10].

A single model input parameter, Fminmax, allows the user of Titan-GRAM or Neptune-GRAM to select where within the min-max envelope a particular simulation will fall. Fminmax = -1, 0, or 1 selects minimum, average, or maximum conditions, respectively, with intermediate values determined by interpolation; i.e., Fminmax between 0 and 1 produces values between average and maximum. Effects such as variation with latitude along a given trajectory path can be computed using the appropriate representation of Fminmax variation with latitude.

Since drag is proportional to density, density is the most important atmospheric parameter for aerocapture. Next most important is height variation of density (as characterized by density scale height). Density scale height is important in determining aerocapture corridor width, or entry angle range that allows the vehicle to achieve capture orbit without "skipping out" or "burning in". As discussed above, small density scale height means rapid change of density with altitude, which results in low corridor width. Large density scale height implies slow density change with altitude, and large corridor width.

Fig. 5 compares height profiles of density scale height among the planets and Titan. Aerocapture altitude (c.f. discussion of Fig. 2) is indicated by letter A in Fig. 5. This figure shows low density scale heights (4-8 km) at aerocapture altitudes for the terrestrial planets. Larger scale heights (≈ 30-50 km) occur at aerocapture altitudes on Neptune and Titan.

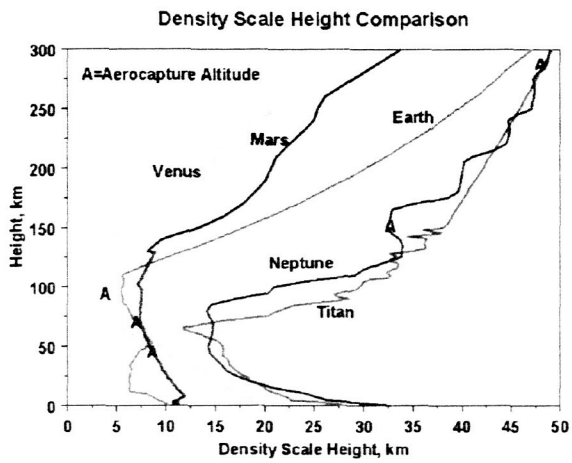

Fig. 5. Comparison of atmospheric density scale height among the planets and Titan

3. TITAN-GRAM GCM OPTION

An option has recently been added for using Titan General Circulation Model (GCM) data as input for Titan-GRAM. The Titan GCM data used are from graphs in [12]. Upper altitudes for the Titan GCM option are computed using a parameterized fit to Titan exospheric temperatures, taken from graphs in [13]. Fig. 6 shows a height-latitude cross section of density, expressed as percent deviation from the mean, for Voyager encounter date November 12, 1980 (planetocentric longitude of Sun Ls = 8.8°), 00:00 GMT, longitude zero, local solar time 0.7 Titan hours. Fig. 7 compares vertical density profiles at latitude zero, local solar time 1 hour and 13 hours on the Voyager encounter date, with the Huygens Yelle [9] minimum-maximum density envelope from Fig. 3. This figure shows that the Titan GCM results correspond fairly closely with Yelle maximum conditions up to about 300 km altitude, and agree quite closely with Yelle average conditions (vertical line at 0 in Fig. 7) above about 500 km.

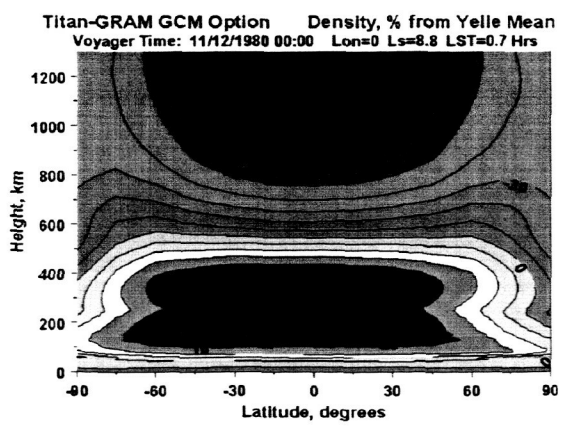

Fig. 6. Density (percent deviation from mean) versus height and latitude, using Titan-GRAM GCM option.

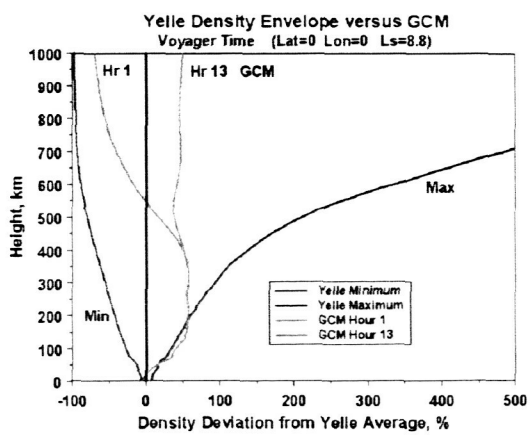

Fig. 7. Comparison of two selected Titan-GRAM density profiles (GCM option) with minimum-maximum envelope from Huygens Yelle model [9].

4. VENUS-GRAM DEVELOPMENT

Based on the Venus International Reference Atmosphere (VIRA) [11], Venus-GRAM is being developed and applied in ongoing Venus aerocapture performance analyses. Fig. 8 shows a plot of density (percent deviation from the mean) versus height and latitude from Venus-GRAM. Conditions in Fig. 8 are for $Ls = 90°$ and local solar time = 12 Venus hours.

Below about 100 km altitude on Venus, we find that temperature, density, and density scale height conditions are very uniform with both latitude and time of day. VIRA data below 100 km altitude vary only slightly with latitude and have no dependence on local solar time. Between 100 km and 150 km, VIRA data depend on local solar time, but not latitude. From 150 km to its top at 250 km, VIRA depends on solar zenith angle, which is affected by both latitude and local solar time.

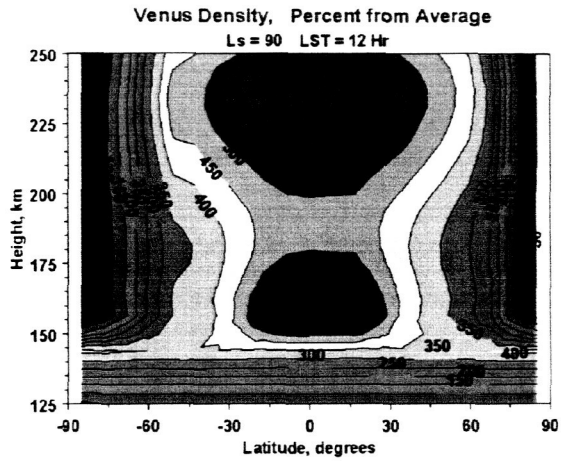

Fig. 8. Example height-latitude density cross section from Venus-GRAM.

5. NEW MARS-GRAM FEATURES

During Mars Global Surveyor (MGS) aerobraking operations, large density variations were observed between successive periapsis passes [14]. These appeared to be longitude-fixed or terrain-fixed waves, usually dominated by wave-2 or wave-3 components (wave-n meaning that n wavelengths fit around a 360° longitude circle). During Mars Odyssey aerobraking, similar large-amplitude density variations were observed. However, during some periods, Odyssey-observed density variations appeared to be traveling waves whose phase speed relative to a fixed longitude seemed to remain constant for a matter of a few days. Mars-GRAM 2001 has an option to represent terrain-fixed waves of the type observed by MGS. Work is underway to develop a new version of Mars-GRAM that will (among other features) include the option to allow user input values for phase speed of traveling wave components, of the type observed by Mars Odyssey.

Also during MGS and Odyssey aerobraking, it was observed that Mars-GRAM produced better correspondence with observed atmospheric density if the altitude scale of its input Mars Thermospheric General Circulation Model (MTGCM) data base was shifted (described as a "height offset"). New sets of Mars General Circulation Model (MGCM) and MTGCM data are being produced for use as input in the next Mars-GRAM update. These GCM model runs include better treatment of the matchup conditions (both mean conditions and upward wave fluxes) between the upper boundary of MGCM and lower boundary of MTGCM (at the 1.32 μbar level, near 80 km). A new non-local thermodynamic equilibrium (non-LTE) method for treating near-infrared heating and CO_2 15-micron cooling will also be employed in the MTGCM model runs. This methodology is based on a non-LTE model of López-Valverde and López-Puertas [15]. More realistic dynamics in both MGCM and MTGCM data sets is also anticipated from the use of latitude and seasonal variations of dust optical depth observed by MGS Thermal Emission Spectrometer (TES) in its mapping years 1 and 2. It is hoped that these new MGCM/MTGCM input data sets for Mars-GRAM will significantly lessen the need for height offset, and significantly improve the correspondence with observed densities during Mars-GRAM use in support of aerobraking operations for Mars Reconnaissance Orbiter.

6. NEW MARS-GRAM SLOPE-WIND FEATURE

For potential applications in preliminary site screening for Mars landers, a new slope wind feature is being developed for Mars-GRAM. Slope winds are computed in Mars-GRAM from a diagnostic (algebraic) relationship based on [16]. This approach differs from mesoscale models, such as Mars Regional Atmospheric Model System (MRAMS) [17], and Mars Mesoscale Model version 5 (MMM5) [18], which use prognostic, full-physics solutions to the time- and space-dependent differential equations of motion. As such, slope winds in Mars-GRAM will be consistent with its

"engineering-level" approach, and will be extremely easy and fast to evaluate, compared with mesoscale model solutions. Mars-GRAM slope winds are not being suggested as a replacement for more sophisticated, full-physics mesoscale models, but may have value, particularly for preliminary screening of large numbers of candidate landing sites for future Mars missions.

Terrain slopes used in the slope wind model are computed from 0.5 x 0.5 degree Mars Orbiter Laser Altimeter (MOLA) topography. Mars-GRAM slope winds will be added to winds from MGCM, which have a resolution of 7.5 x 9 degrees in latitude and longitude. The Mars-GRAM slope wind model will thus add significantly higher resolution information about possible near-surface winds than is provided by MGCM.

Fig. 9 shows Mars-GRAM slope winds, evaluated at a level 2 km above local terrain height for the Gusev Crater area, at the date and time of Rover Spirit landing. If this wind field is valid, then Spirit would have experienced up to ~ 25 m/s winds "opposing" its entry into Gusev Crater near an altitude of 1-2 km above surface level. Spirit experienced significant turbulence or winds during its descent (Prasun Desai, private communication), causing it to fire its Transverse Impulse Rocket System to correct for off-vertical firing of its main retrorockets, and to reduce its lateral impact speed.

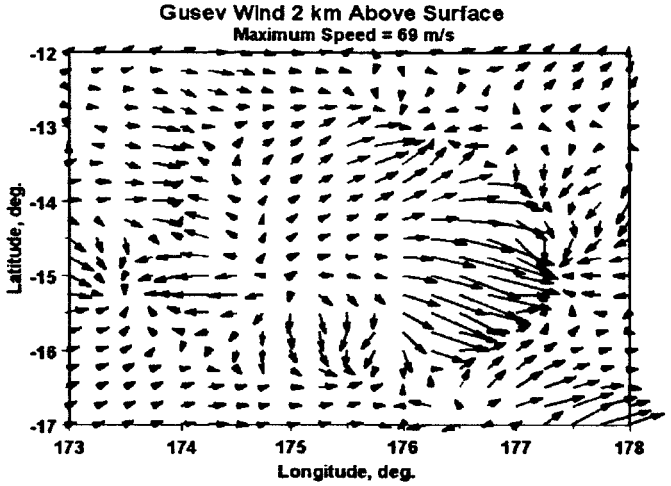

Fig. 9. Slope wind vectors at Gusev Crater, 2km above surface, for date and time of Spirit landing.

Fig. 10 shows MOLA terrain heights in a portion of the eastern end of Valles Marineris, used in these preliminary tests of the slope wind model. Fig. 11 shows northward component of Mars-GRAM slope winds, evaluated at a level 1 km above local terrain height for the study area shown in Fig. 10. The season assumed is Ls = 0 (northern spring equinox) at local time 14 hours. Comparison of Fig. 11 with Fig. 10 shows that the major pattern for slope winds at this time is northward and upward along the north wall of the valley and southward and upward along the south wall (i.e. upslope flow on both valley walls), a reasonable situation for early afternoon local time. These examples of test output from the new Mars-GRAM slope wind model may be compared with wind simulations from Mars mesoscale models, presented by Rafkin and Michaels [19] and Kass, et al. [20].

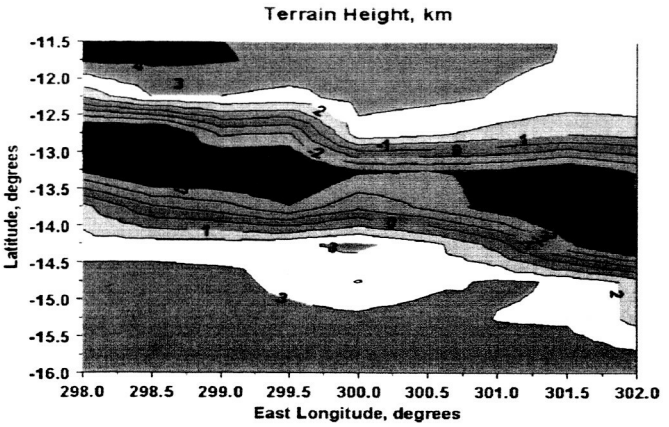

Fig. 10. Terrain Heights in portion of Valles Marineris region

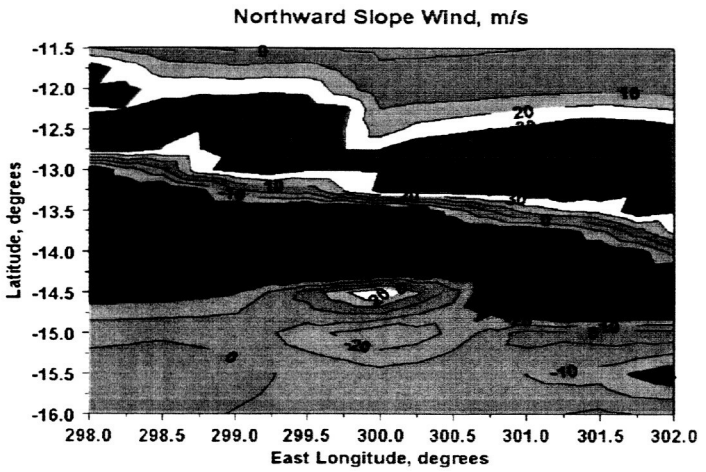

Fig. 11. Northward slope winds at Ls = 0 and LST = 14 hours, 1km above terrain surface.

7. PERTURBATION MODELS

An important feature of all the GRAM atmospheric models is their ability to simulate "high frequency" perturbations in density and winds, due to such phenomena as turbulence and various kinds of atmospheric waves. As illustrated in Fig. 12, Earth-GRAM altitude, latitude, and monthly variations of perturbation standard deviations are based on a large climatology of observations. For Titan-GRAM and Neptune-GRAM, perturbation standard deviations are computed from an analytical expression for gravity wave saturation conditions, explained more fully in [7]. As shown in Fig. 12, the resulting vertical profiles of standard deviations for Titan and Neptune are not dissimilar to Earth observations, when expressed as percent of mean density. For Mars-GRAM, a similar gravity wave saturation relation is used to estimate density perturbation standard deviations, except that effects of significant topographic variation on Mars are also taken into account. Up to about 75 km altitude, the Mars model density standard deviations are also fairly consistent with Earth observations. By about 100 km to 130 km altitude, Mars model density standard deviations increase to about 20% to 35% of mean value, consistent with observed orbit-to-orbit density variations observed by Mars Global Surveyor and Mars Odyssey.

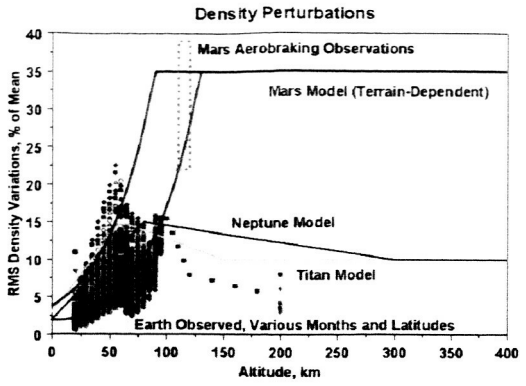

Fig. 12. Height variation of density perturbation model standard deviations for Earth, Mars, Titan, and Neptune.

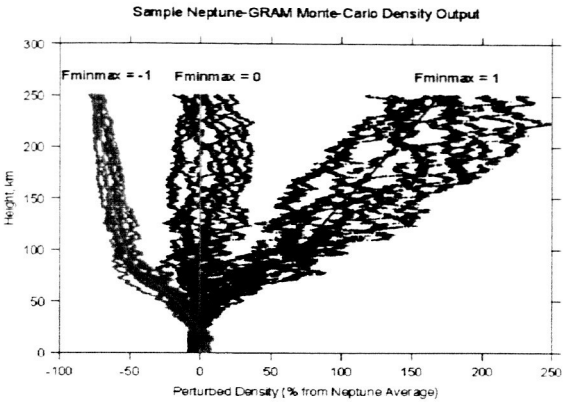

Fig. 13. Sample Monte Carlo density perturbations from Neptune-GRAM, expressed as percent deviation from Neptune mean value.

A typical application of the Neptune-GRAM perturbation model is shown in Fig. 13. Neptune-GRAM was recently utilized in Neptune aerocapture systems analysis studies. The chosen aerocapture design reference mission included simulations which involved capture into a highly eccentric orbit, to allow the orbiter to periodically visit Triton for scientific observations. The ability to successfully aerocapture into such an eccentric orbit depends very significantly on details of Monte Carlo trajectory simulations, particularly on atmospheric density variations such as illustrated in Fig 13. For such an eccentric orbit, there is relatively little margin for error between a captured orbit and one which exceeds escape velocity upon atmospheric exit, a result which could ultimately lead to mission failure. Neptune-GRAM was used to define an aerocapture corridor width consistent with mission success.

8. CONCLUSIONS

The engineering-level atmospheric models presented here are suitable for a wide range of mission design, systems analysis, and operations tasks. For orbiter missions, applications include analysis for aerocapture or aerobraking operations, analysis of station-keeping issues for science orbits, analysis of orbital lifetimes for end-of-mission planetary protection orbits, and atmospheric entry issues for accidental break-up and burn-up scenarios. For lander missions to Venus, Mars and Titan, and for Earth-return, applications include analysis for entry, descent and landing (EDL), and guidance, navigation and control analysis for precision landing and hazard avoidance. Perturbation simulation capabilities of these models make them especially useful in Monte Carlo analyses for design and testing of guidance, navigation, and control algorithms, and for heat loads analysis of thermal protection systems.

9. ACKNOWLEDGMENTS

The authors gratefully acknowledge support from the NASA Marshall Space Flight Center In-Space Propulsion Program. Particular thanks go to Bonnie James (MSFC), Manager of the Aerocapture Technology Development Project, to Michelle M. Munk (LaRC/MSFC), Lead Systems Engineer for Aerocapture, and to Melody Herrmann (MSFC), team lead and Mary Kae Lockwood (LaRC), technical lead for the Titan/Neptune Systems Analysis study. Model user feedback and suggestions from the following individuals are also greatly appreciated: Dick Powell, Brett Starr, and David Way (NASA LaRC), and Claude Graves, Jim Masciarelli, Lee Bryant, Tim Crull, and Tom Smith (NASA JSC). External review comments from Prof. Darrell Strobel (Johns Hopkins University) were especially helpful.

10. REFERENCES

1. Justus, C. G., and Johnson, D. L., "The NASA/MSFC Global Reference Atmospheric Model - 1999 Version (GRAM-99)", NASA/TM-1999-209630, 1999.

2. Justus, C.G., Duvall, A. L., and Johnson, D. L., "Earth Global Reference Atmospheric Model and Trace Constituents", *34th COSPAR Scientific Assembly*, Houston, Texas, Invited Paper C4.1-0005-02, October, 2002.

3. Justus, C. G., and Johnson, D. L., "Mars Global Reference Atmospheric Model 2001 Version (Mars-GRAM 2001) Users Guide", NASA/TM-2001-210961, April, 2001.

4. Justus, C. G., Duvall, A. L., and Johnson, D. L., "Mars-GRAM Validation with Mars Global Surveyor Data", *34th COSPAR Scientific Assembly*, Houston, Texas, Paper C3.3-0029-02, October, 2002.

5. Justus, C. G., Duvall, A. L., and Johnson, D. L., "Global MGS TES Data and Mars-GRAM Validation", *34th COSPAR Scientific Assembly*, Houston, Texas, Paper C4.2-0005-02, October, 2002.

6. Justus, C. G., Duvall, A. L. and Johnson, D. L., "Mars Global Reference Atmospheric Model (Mars-GRAM) and Database for Mission Design", *International Workshop on Mars Atmosphere Modeling and Observations*, Granada, Spain, January, 2003.

7. Justus, C.G., Duvall, A. L., and Johnson, D. L., "Engineering-level model atmospheres for Titan and Neptune", *39th AIAA/ASME/SAE/ASEE Joint Propulsion Conference*, Huntsville, Alabama, Paper AIAA-2003-4803, July, 2003.

8. Justus, C.G., Duvall, A. L., and Keller, V. W., "Engineering-level model atmospheres for Titan and Mars", *International Workshop on Planetary Probe Atmospheric Entry and Descent Trajectory Analysis and Science*, Lisbon, Portugal. October, 2003.

9. Yelle, R.V. , Strobell, D. F., Lellouch, E., and Gautier, D., " Engineering Models for Titan's Atmosphere", in *Huygens Science, Payload and Mission*, ESA SP-1177, August, 1997.

10. Cruikshank, D.P. (ed.), *Neptune and Triton*, University of Arizona Press, Tucson, 1995.

11. Kliore, A. J., Moroz, V. I., and Keating, G. M. (eds.), "The Venus International Reference Atmosphere", *Advances in Space Research*, vol. 5, no. 11, 1985, Pergamon Press, Oxford, 1986, pp. 1-304.

12. Hourdin, F., Talagrand, O., Sadourny, R., Courtin, R., Gautier, D., and McKay, C.P., "Numerical simulation of the general circulation of the atmosphere of Titan", *Icarus*, vol. 117, no. 2, Oct. 1995, pp. 358-74.

13. Mueller-Wodarg, I. C. F., "The Application of General Circulation Models to the Atmospheres of Terrestrial-Type Moons of the Giant Planets", in *Comparative Atmospheres in the Solar System*, American Geophysical Union, 2002.

14. Keating, G.M., Bougher, S. W., Zurek, R. W., Tolson, R. H., Cancro, G. J., Noll, S. N., Parker, J .S., Schellenberg, T. J., Shane, R. W., Wilkerson, B. L., Murphy, J. R., Hollingsworth, J. L., Haberle, R. M., Joshi, M., Pearl, J. C., Conrath, B J., Smith, M. D., Clancy, R .T., Blanchard, R. C., Wilmoth, R. G., Rault, D. F., Martin, T. Z., Lyons, D. T., Esposito, P. B., Johnston, M. D., Whetzel, C. W., Justus, C. G., Babicke, J. M., "The structure of the upper atmosphere of Mars: in situ accelerometer measurements from Mars Global Surveyor", *Science*, **279**(5357), 1672-6, 1998.

15. López-Valverde, M. A. and López-Puertas, M., "A non-local thermodynamic equilibrium radiative transfer model for infrared emissions in the atmosphere of Mars. 1. Theoretical basis and nighttime populations of vibrational states", *Journal of Geophysical Research*, **99**, 13, 093-13,115, 1994.

16. Ye, Z. J., Segal, M., and Pielke, R. A., "A comparative study of daytime thermally induced upslope flow on Mars and Earth", *Journal of the Atmospheric Sciences*, **47**(5), 612-628, 1990.

17. Rafkin, S. C. R., Haberle, R. M., and Michaels, T. I., "The Mars Regional Atmospheric Modeling System: model description and selected simulations", *Icarus*, **151**, 228-256, 2001.

18. Toigo, A. D., and Richardson, M. I., "A mesoscale model for the Martian atmosphere", *Journal of Geophysical Research*, **107**(E7), 3-1-21, 2002.

19. Rafkin, S. C. R. and Michaels, T. I., "Meteorological predictions for 2003 Mars Exploration Rover high-priority landing sites", *Journal of Geophysical Research*, **108**(E12), 32-1-22, doi:10.1029/2002JE002027, 2003.

20. Kass , D. M., Schofield, J. T., Michaels, T. I., Rafkin, S. C. R., Richardson, M. I., and Toigo, A. D., "Analysis of atmospheric mesoscale models for entry, descent, and landing", *Journal of Geophysical Research*, **108**(E12), 31-1-10, doi:10.1029/2003JE002065, 2003.